DYNAMIC STRENGTH TESTING OF PERFORATED STEEL - GRP DOUBLE LAP JOINTS

R. J. Brambleby*[1], L. A. Louca[1], S. E. Mouring[2]

[1] *Civil & Environmental Engineering, Imperial College London, South Kensington, London SW7 2AZ*
[2] *U.S. Naval Academy, Naval Arch. and Ocean Engr., 590 Holloway Rd., Annapolis, MD 21402*
* *Corresponding Author: reuben.brambleby10@imperial.ac.uk*

Keywords: hybrid joint, dynamic strength, vinyl ester, stainless steel,

Abstract
Joints between metals and composites are being employed in a range of applications, but the performance of such joints under dynamic loading is not well documented. This paper presents some initial results investigating the tensile strength of steel to GRP double lap joints comparing pseudo static strength with dynamic strength and comparing joints that have non-perforated steel plates with joints that have perforated steel plates. The effect of an intentional manufacturing flaw is also considered. It has been observed that the strength enhancement provided by the perforations is significant, but marginally lower under dynamic loading than under static loading.

1. Introduction

Joints between metals and composite materials are being employed in a range of applications within sectors including marine, energy and transportation. The performance of such joints under dynamic loading is not well documented. This paper presents some initial results from tensile strength testing of steel to vinyl ester GRP double lap joints, comparing pseudo static strength with dynamic strength and comparing joints that exploit perforated steel plates with those manufactured with non-perforated steel plates. An intentional manufacturing flaw was also incorporated into half of the joints, both perforated and non-perforated, in order to assess the effect of this flaw type on joint strength. The dynamic tensile loading is applied to the joints using an impact tension adapter designed by the research group at Imperial College London. It has been observed that the enhancement in static strength which can be gained by exploiting perforated steel plates can also be gained under dynamic loading, although the enhancement under dynamic loading is marginally lower.

2. Specimen Design

This study is an extension of work reported by Melograna & Grenestedt [1] in which double lap joints between steel and vinyl ester GRP were tested under static loading. The effect of various steel perforation geometries were examined including circular perforations with graduated diameters. The perforations near the tip of the steel plate have the largest diameter and the perforation diameter reduces as distance from the tip of the plate increases, see Figures 1(a)

& 2. A significant effect of this variation in diameter is to gradually increase the effective axial stiffness of the steel plate and thus to mitigate the effects of stiffness mismatch between the GRP and steel materials.

Although the design of the strongest joint reported by Melograna & Grenestedt [1] was the starting point for the design the joints here, the steel material that was readily available for this study was thinner and of a lower strength than the steel used by Melograna & Grenestedt. Thus a shorter lap length was used here, 40mm rather then 50mm, in order to ensure that failure would occur in the joints themselves rather than in the steel plate beyond the joint. The number of rows of perforations was correspondingly reduced from 9 to 8. The geometry for the remainder of the specimen beyond the joint itself, see Figure 2, is dictated by the Impact Tension Adapter (ITA) loading device which is described in Section 3.2.

Figure 1(b) shows the laminate layup that was used for the GRP portion of the joints. The TTX1330 is an Owens Corning (OCV) stitched triple ply S2 glass fabric with an overall areal density of 1330 g/m^2. Laminates 1 & 4 become the 40mm long laps which form the joint with the steel plate. The M8610 continuous fibre mat placed at the mid thickness of the layup is provided as a non-structural filler material which permits laminates 1 & 4 to have a smooth transition onto the steel plate. Beyond the instrumented portion of the specimen two additional layers of TTX1330, laminates 0 & 5, provide the additional thickness required for the ITA bottom clamps.

The intentional fabrication flaws were generated by applying semi-circular pieces of single sided self adhesive PTFE tape to both sides of the steel plate prior to fabrication of the specimen, these flaws are indicated in Figure 3. The materials used for the specimens in this study are given in Table 1.

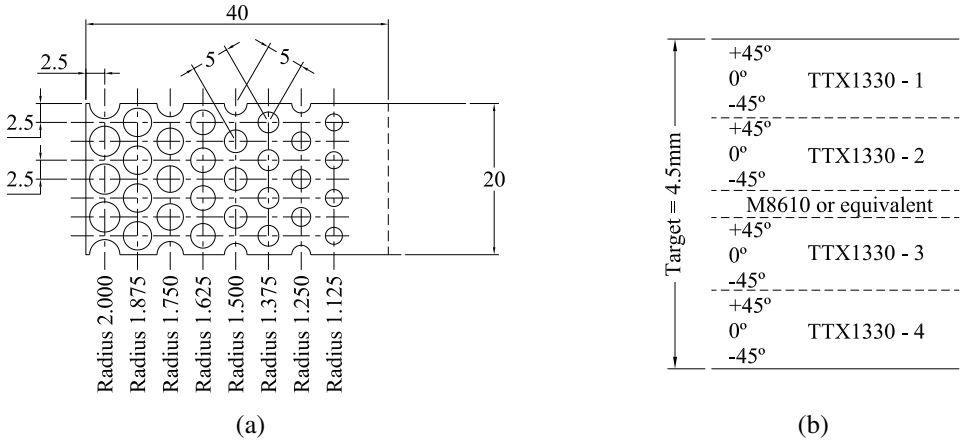

Figure 1. (a) Steel plate perforation geometry and (b) GRP laminate layup used in this study.

3. Experimental Test Method

3.1. Pseudo Static Testing

Half of the specimens were tested with pseudo-static tensile loading in order to determine a base-line strength and base-line failure behaviour against which the dynamically loaded specimens can be compared. The pseudo-static tests were carried out with a crosshead displacement

Function	Material Used	Description
GRP Resin	Dow Derakane 510A-40	Epoxy Vinyl Ester Resin
GRP Reinforcement	Owens Corning TTX1330	Stitched glass fabric, +45°, 0°, -45°
GRP Filler	Owens Corning M8610	Glass fibre, continuous filament
Steel Plate	3/32" thick, grade 304	Stainless steel

Table 1. Materials used to fabricate the joint specimens.

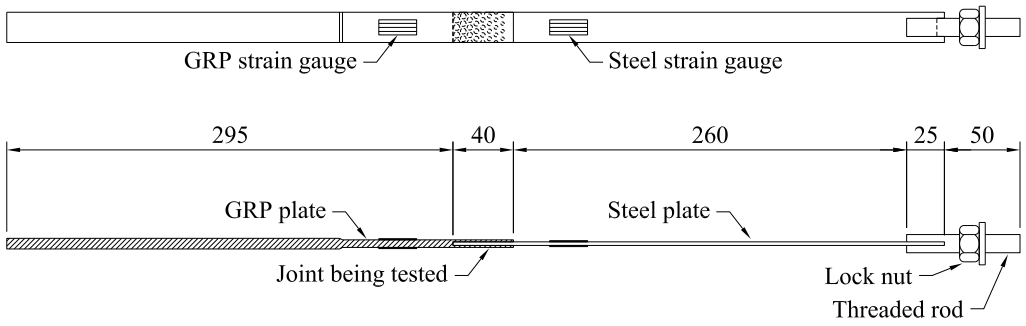

Figure 2. Overall geometry of the specimens used in this study.

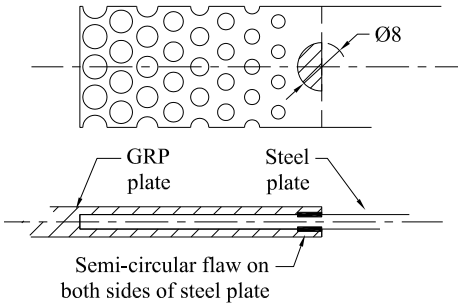

Figure 3. Intentional flaw applied to half of the specimens.

rate of 1mm/min in an Instron uni-axial twin screw test machine fitted with a 2580 series static load cell. Strain gauges were applied to the GRP portion of the static specimens in order to measure strain in the GRP plates beyond the joint itself, see Figure 2. Measurement data was recorded from the strain gauges, the load cell and the crosshead displacement transducer. The data acquisition equipment comprised a Fylde FE-H379-TA high speed transducer amplifier and a windows PC workstation fitted with a high speed data acquisition card. For the static testing the data acquisition rate was 1kHz which is the lowest rate available on the card. Figure 4(a) shows a specimen ready to be tested under static loading.

3.2. Dynamic Testing

The remaining half of the specimens were tested with dynamic tensile loading in order to expose differences, in terms of tension strength and failure behaviour of the joint, under a higher rate of loading. The dynamic load is generated in an Instron Dynatup 9200 drop weight test rig. The impact load generated by this rig is converted into a dynamic tension load using an Impact Tension Adapter (ITA) designed and manufactured at Imperial College London, the operation

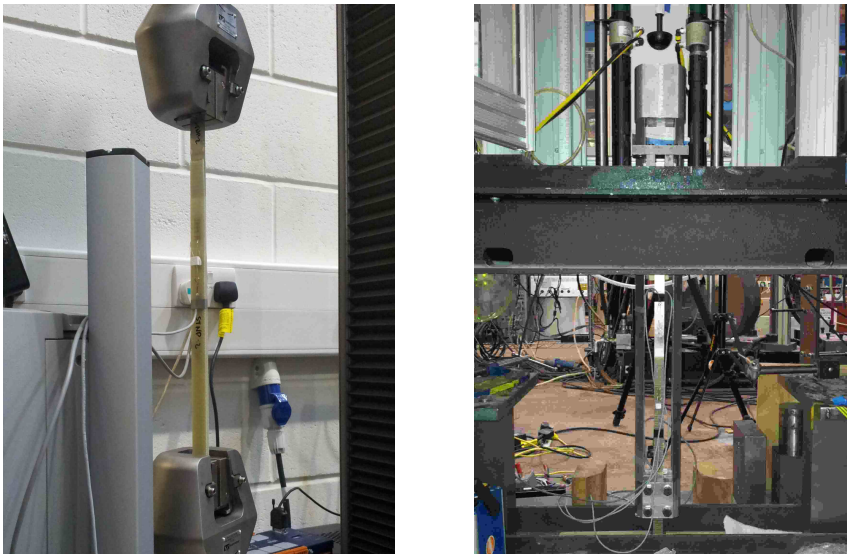

(a) Static tension rig. (b) ITA within the drop weight rig.

Figure 4. Specimens in the static and dynamic test rigs ready for testing.

of the ITA is described in Figure 5. The drop weight mass used in this study was approximately 5.2kg and the impact energy was approximately 45J.

Strain gauges were applied to both the GRP and steel portions of the specimen as shown in Figure 2. Measurement data from the strain gauges, impact tup load cell and ITA accelerometer was recorded throughout the test with a data acquisition rate of 10MHz. The accelerometer was fixed to the upper surface of the bottom yoke of the ITA. Figure 4(b) shows a specimen ready to be tested under dynamic loading.

3.3. Coupon Testing

Tension tests have been carried out for coupons of both the steel and GRP material used here in order to determine the strain versus stress relationships for the two materials. This was necessary due to the fact that a load cell is not incorporated into the dynamic test setup and the load in the specimen must be calculated using the strains measured during the dynamic tests. The pseudo static coupon tests were carried out at an extension rate of 1mm/min. The averaged results were used to generate polynomial expressions relating strain and stress. These expressions were subsequently used to calculate specimen load from measured strains.

It was found that the perforated joints were strong enough to generate significant plastic deformation in the steel plate. The stress strain relationship of the steel is significantly strain rate dependent [2] while the stress strain relationship for the GRP is much less strain rate dependent at the values of strain generated in this study [3]. For this reason the GRP strain measurements are used to calculate the instantaneous joint load in the dynamic tests.

4. Results

A summary of the measured failure loads is given in Table 2. The mean value of failure load is given for each of the four types of specimen under the two types of loading. The scatter for each

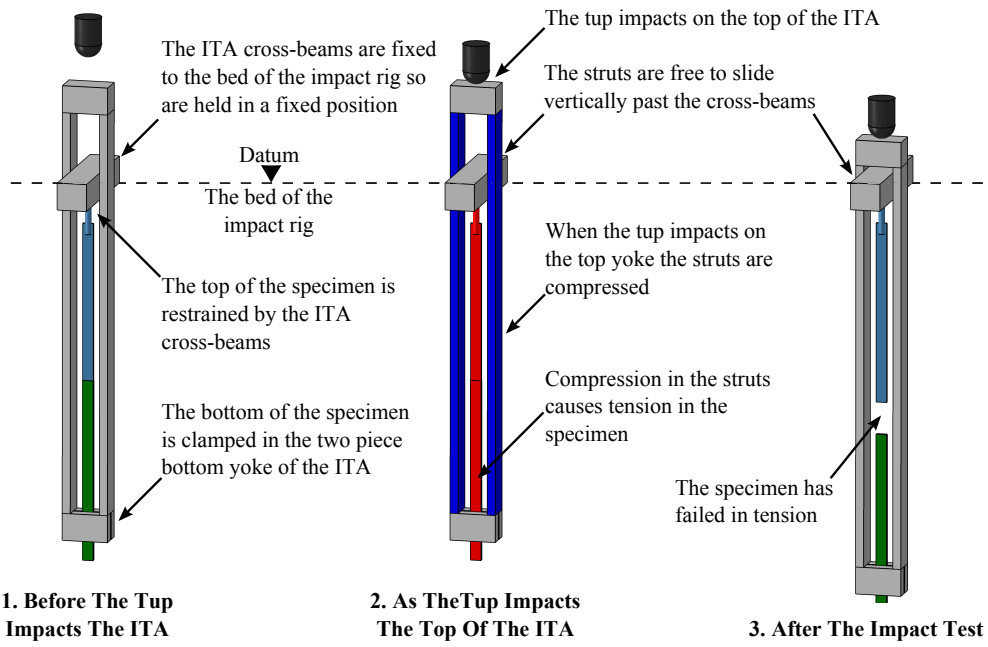

Figure 5. Operation of the Impact Tension Adapter (ITA).

	Static Loading		**Dynamic Loading**	
	Mean	Spread	Mean	Spread
Perforated No Flaw	**10.8**	±3%	**15.2**	±15%
Perforated With Flaw	**11.0**	±5%	**14.9**	±1%
Non-perforated No Flaw	**4.4**	±56%	**6.2**	±2%
Non-perforated With Flaw	**4.5**	±32%	**6.6**	±6%

Table 2. Summarised results - mean failure load (kN) for each specimen type.

value is also quoted as a percentage of the corresponding mean value. It should be noted that in most cases each value given in Table 2 represents only 3 individual specimens. Typical load versus extension plots for both perforated and non-perforated statically loaded specimens are given in Figure 6. Extension in this case is the test machine crosshead displacement. Typical load versus extension plots for both perforated and non-perforated dynamically loaded specimens are given in Figure 7. Extension in this case is calculated by double integration of the acceleration of the ITA bottom yoke. Representative strain rates in the steel and GRP portions of a dynamically loaded perforated specimen are quoted in Figure 8.

From the high speed video images captured during the tests, it is evident that in all specimens under both static and dynamic loading the failure initiates at the tip of the steel plate. Figure 9 shows selected video frames captured during the test of a typical dynamically loaded perforated joint specimen and Figure 8 shows where these frames occurred in relation to the strain versus time plot. Figure 9(a) shows an unmodified image, a high pass filter has been applied to the remaining images in order to accentuate the damaged area which can be difficult to distinguish in still images.

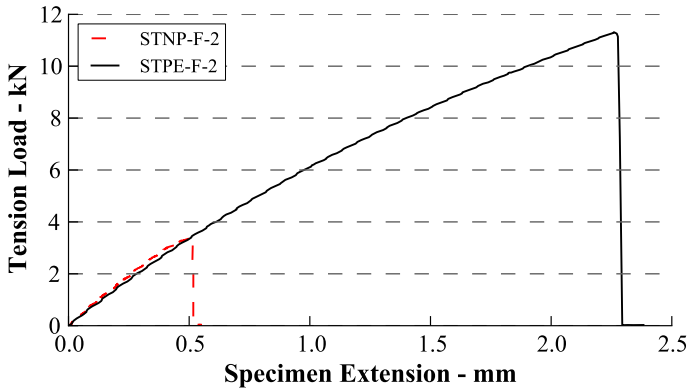

Figure 6. Typical load versus extension plots for static loading of perforated (STPE) and non-perforated (STNP) joints.

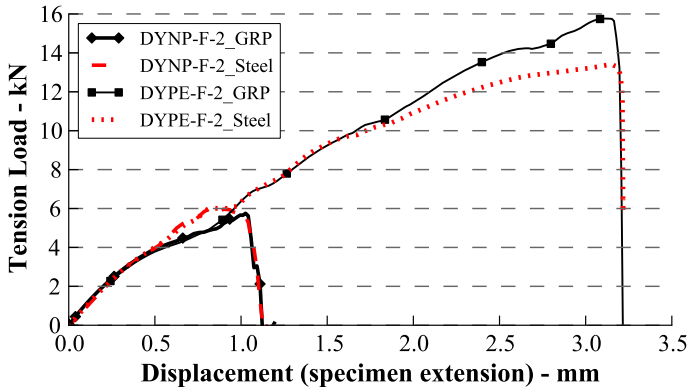

Figure 7. Typical Load versus displacement plots for dynamic loading of perforated (DYPE) and non-perforated (DYNP) joints. The load calculated from both GRP and steel strains are plotted.

Referring to Figure 9 the failure process for the perforated joints can be described as follows:

- Frame 150 - Just prior to load being applied.
- Frame 206 - De-bond failure initiates at the tip of the steel plate, the darkened area.
- Frame 230 - De-bonding spreads extending in both directions, i.e. along the steel plate and into the solid GRP plate. De-bonding from the steel plate is almost complete but the bond with the resin in the perforations remains largely intact.
- Frame 236 - The joint has failed, the GRP and steel portions have become separated.

5. Discussion

As expected from the results of Melograna & Grenestedt [1], the perforated joints have a significantly higher strength than the non-perforated joints, with an enhancement factor of 2.46 under static loading and 2.35 under dynamic loading. The scatter in the results is significantly higher for the non-perforated joints. It seems likely that this increased scatter can be attributed to random unintentional variations in the fabrication process and in particular to the preparation of the steel bonding surface. In all cases the preparation for the steel bonding surface was

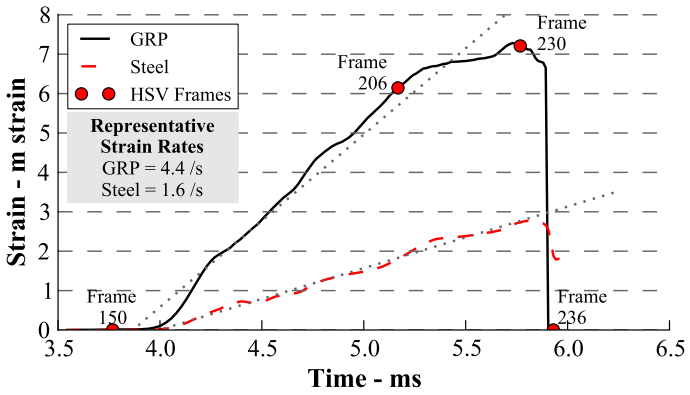

Figure 8. Time versus strain plot for dynamically loaded perforated joint specimen DYPE-3. The frame numbers relate to the high speed video frames in Figure 9.

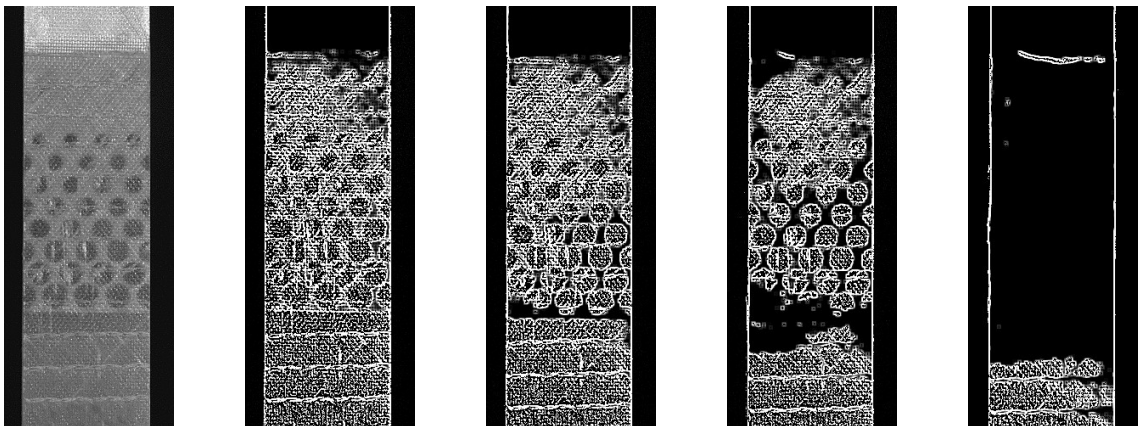

(a) Frame 150 (b) Frame 150 (c) Frame 206 (d) Frame 230 (e) Frame 236

Figure 9. Individual frames from the high speed video recording of the dynamic test on specimen DYPE-3.

simply grit blasting and de-greasing. It is possible that these manual processes cause significant variability in the performance of the non-perforated joints.

The results in Table 2 show that the flaw had negligible effect on the strength for both perforated and non-perforated joints. Failure of all specimens initiated at the tip of the steel plate while the de-bond flaws are placed below the tip of the GRP cover plates. It is likely that if the flaws were placed at the opposite end of the joint, near the tip of the steel plate, then their influence on joint strength would be greater.

The dynamic strength of the joints is higher than the static strength, by a factor of 1.44 for the non-perforated joints and a factor of 1.37 for the perforated joints. The reasons for this general increase in strength are unclear at this stage. However, it can be seen from a literature search that strain rate does influence both mode I and mode II interlaminar fracture toughness of epoxy resins. For example Kusaka et al [4] report that an increase in loading rate leads to a decrease in mode I interlaminar fracture toughness for carbon reinforced epoxy resin, while Carlberger et al [5] report that an increase in loading rate leads to an increase in mode I and a decrease in mode II fracture toughness for epoxy adhesive. It is possible that the influence of strain rate

on resin performance is contributing to the higher joint strengths at the higher loading rate, that were observed in this study.

6. Conclusions & Further Work

The behaviour of perforated and non-perforated steel to GRP double lap joints under tension loading have been investigated for both pseudo static loads and impact loads. It has been found that both perforated and non-perforated joints are significantly stronger under dynamic tension loads than pseudo-static tension loads. This increase in strength is slightly less significant for perforated joints than for non-perforated joints.

With the aim of determining the origin of the apparent increase in strength of the joints under dynamic loading we plan to:

- Carry out coupon tests on the GRP and steel materials at higher loading rates.
- Investigate mode II fracture toughness for GRP-GRP and GRP-Steel interfaces at a range of loading rates.
- Investigate the dynamic tension behaviour of the joints using finite element models.

7. Acknowledgements

The authors would like to thank the team at TSD, Project Support Branch, US Naval Academy under the guidance of Mr Doug Loup, Naval Suface Warfare Center Carderock Division for fabricating the specimens used in the experiments, Office of Naval Research for funding the project and Andy Pullen at Imperial College London for his assistance in the experimental work.

References

[1] J. D. MELOGRANA and J. L. GRENESTEDT. Improving joints between composites and steel using perforations. *Composites Part A: Applied Science and Manufacturing*, 33(9):1253–1261, 2002.

[2] J. A. LICHTENFELD, C. J. TYNE, and M. C. MATAYA. Effect of strain rate on stress-strain behavior of alloy 309 and 304l austenitic stainless steel. *Metallurgical and Materials Transactions A*, 37(1):147–161, 2006.

[3] B. A. GAMA, J. W. GILLESPIE, H. MAHFUZ, R. P. RAINES, A. HAQUE, S. JEELANI, T. A. BOGETTI, and B. K. FINK. High strain-rate behavior of plain-weave s-2 glass/vinyl ester composites. *Journal of Composite Materials*, 35(13):1201–1228, 2001.

[4] T. KUSAKA, M. HOJO, YW. MAI, T. KUROKAWA, T. NOJIMA, and S. OCHIAI. Rate dependence of mode i fracture behaviour in carbon-fibre/epoxy composite laminates. *Composites Science and Technology*, 58(3-4):591–602, 1998.

[5] T. CARLBERGER, A. BIEL, and U. STIGH. Influence of temperature and strain rate on cohesive properties of a structural epoxy adhesive. *International Journal of Fracture*, 155(2):155–166, 2009.